Light-load Efficiency Enhancement of High-Frequency Dual-Active-Bridge Converter Under SPS Control

Chen, Xiaoying; Xu, Guo; Han, Hua; Liu, Dong; Sun, Yao; Su, Mei

Published in:
IEEE Transactions on Industrial Electronics

DOI (link to publication from Publisher):
10.1109/TIE.2020.3044803

Publication date:
2021

Document Version
Accepted author manuscript, peer reviewed version

Light-load Efficiency Enhancement of High-Frequency Dual-Active-Bridge Converter Under SPS Control

Xiaoying Chen, *Student Member, IEEE*, Guo Xu, *Member, IEEE*, Hua Han, Dong Liu, *Senior Member, IEEE*, Yao Sun, *Member, IEEE*, and Mei Su, *Member, IEEE*

***Abstract*—Dual-active-bridge (DAB) converter is an attractive topology to be used as a DC transformer (DCT) in the DC power distribution system. Because the voltage gain for DC transformer is relatively fixed, single-phase-shift (SPS) control is popularly adopted for DAB converter to achieve simple power control. Aiming at increasing the light load efficiency of high-frequency DAB converter under SPS control, this letter proposes a concept to achieve full load range zero-voltage-switching (ZVS) with minimum RMS current in certain voltage variation range. In the proposed method, the added magnetizing inductance creates the possibility to achieve ZVS for all power switches. And, the voltage gain of the converter is specially controlled by turns ratio, which is no longer the conventional unity voltage gain condition. The key parameters optimization, including the turns ratio, magnetizing inductance and leakage inductance of the transformer, are introduced based on ZVS and current stress analysis. A 250 kHz, 400/48V, 1000W GaN-based DAB prototype is built, which shows performance improvements at light load.**

***Index Terms*— Dual-Active-Bridge, SPS control, Full load range ZVS**

I. Introduction

Using an isolated bidirectional dc-dc converter as a DC transformer (DCT) is an attractive solution to achieve power flow balance between two DC buses of the DC power distribution system [1]. In view of the converter topology, dual-active-bridge (DAB) converter is popularly regarded as the constituent unit of DCT [2], because of few passive components, symmetric structure, and soft-switching capability.

The variations of two bus voltages are small in these DCT applications [3][4], so single-phase-shift (SPS) control is widely used to obtain simple implementation. However, under unity voltage gain condition which is to design the transformer turns ratio n to be equal to $V_1/2V_2$ (as the topology in Fig.1), even though DAB converter has high performance with SPS control, it still suffers from hard switching at light load [5]. These will decrease the light load efficiency, especially when the switching frequency is pushed to high with the development of the wide bandgap semiconductors. Therefore, ZVS at light load is worthy of attention in high-frequency applications.

To solve that problem, compared with SPS control, the control degrees of freedom can be increased, such as extended-phase-shift (EPS) [6], dual-phase-shift (DPS) [7] and triple-phase-shift (TPS) [8]. However, these modulations have multiple control variables, which leads to complex calculations and even hard to achieve unified control. Meanwhile, this will make the DCT lose the benefit of easy implementation which is favored in industrial applications. In literature, no academic paper has been reported to utilize SPS control to achieve full load range ZVS when considering junction capacitors. Actually, based on ZVS analysis in this letter (Section III.B), it is impossible for conventional DAB converter which ignores the magnetizing inductance to achieve full load range ZVS under SPS control. In [9] and [10], the magnetizing inductance is considered to enhance the ZVS range. However, how to design the control algorithm with consideration of this phenomenon and how to make the tradeoffs for the design parameters have not been discussed. In [11], the adjustable-tap transformer is presented to extend the ZVS range and improve the efficiency of the DAB converter. However, full load range ZVS cannot be realized for this method, and hard switching still occurs at light load. In [12], a DC blocking capacitor and a hybrid modulation strategy are used to extend the ZVS range and improve the efficiency at light load. However, there are still some regions cannot achieve ZVS for this method.

In this letter, to improve efficiency at light load, a design concept is proposed for DAB converter to achieve full load range ZVS for all switches in a certain voltage variation range with simple SPS control in DCT applications. The contributions of this letter can be summarized as follows.

(1) This method provides a new view for the DAB converter designed in DCT applications. Instead of designing the rated operating point at unity voltage gain, it purposely designs the voltage ratio a bit away from the unity gain to achieve full load range ZVS.

(2) With proper design of the magnetizing current in the transformer and the non-unity voltage gain conditions, full load range ZVS can be completely realized for all switches considering the switch junction capacitors.

Manuscript received August 24, 2020; revised October 31, 2020; accepted November 24, 2020. This work was supported in part by the Nature Science Foundation of China under Grant 51907206 and 61933011, the Hunan Provincial Key Laboratory of Power Electronics Equipment and Grid under Grant 2018TP1001, the CRRC Zhuzhou Electric Locomotive Institute Co., Ltd.(YJYJS2018-017). (Corresponding author: *Guo Xu*).

X. Chen, G. Xu, H. Han, Y. Sun and M. Su are with the School of Automation, Central South University and with Hunan Provincial Key Laboratory of Power Electronics Equipment and Grid, Changsha, 410083, China, (e-mail: chenxiaoying01@csu.edu.cn; xuguocsu@csu.edu.cn; hua_han@126.com; yaosuncsu@gmail.com; sumeicsu@csu.edu.cn).

Dong Liu is with the Department of Energy Technology, Aalborg University, 9220 Aalborg, Denmark (e-mail: dli@et.aau.dk).

(3) The comprehensive parameter design consideration, including the turns ratio, magnetizing inductance, and leakage inductance of the transformer, is presented with the purposes of achieving both full load range ZVS and small RMS current.

II. Basic Concept of the Proposed Method

A half-bridge DAB converter is used to illustrate the basic concept of the proposed method as shown in Fig.1. And the magnetizing inductor of the transformer is specially addressed.

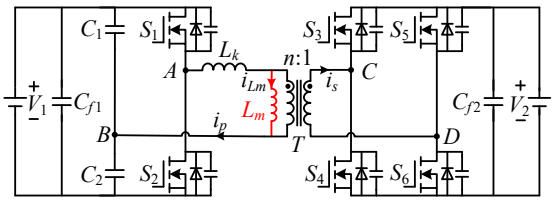

Fig. 1. The topology of DAB converter

To achieve ZVS, the energy stored in the inductive components should be enough to charge/discharge the switch junction capacitors when the switches are turned off. Fig.2 shows the operating waveforms of DAB converter under SPS control. i_{min_p} and i_{min_s} are the threshold current for primary side switches and secondary side switches to achieve ZVS. i_{p_p} at t_4 and i_{p_s} at t_2 are the turn off current of two sides switches. When the turn off current i_{p_p} and i_{p_s} are larger than the threshold current i_{min_p} and i_{min_s} respectively, the switches can achieve ZVS.

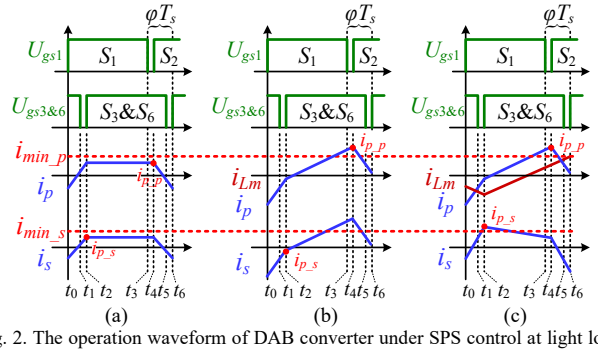

Fig. 2. The operation waveform of DAB converter under SPS control at light load. (a) Unity voltage gain ($n=V_1/2V_2$). (b) Voltage mismatching ($n<V_1/2V_2$). (c) Proposed method ($n<V_1/2V_2$, and considering magnetizing inductor).

Fig.2(a) shows the light-load waveforms under SPS control for the conventional DAB converter which is worked under unity voltage gain ($n = V_1/2V_2$). As seen, the turn off current i_{p_p} at t_4 and i_{p_s} at t_2 are all small than the threshold current i_{min_p} and i_{min_s}, which means both two sides switches cannot achieve ZVS. This can explain the reason of hard switching for SPS control at light load.

In order to achieve ZVS at light load and make i_{p_p} to be larger than the threshold current i_{min_p}, the turns ratio n can be designed to be smaller than $V_1/2V_2$ ($n < V_1/2V_2$). As seen in Fig.2(b), when $n < V_1/2V_2$, the slope of i_p can be increased, and the turn off current i_{p_p} at t_4 will be increased to be larger than the threshold current i_{min_p}, which will help primary side switches to be achieved ZVS at light load.

However, the existing slope in secondary current will lead to hard switching for secondary side switches. As Fig.2(b) shows, at t_2, the turn off current i_{p_s} of the secondary side switches becomes negative, which will cause hard switching for secondary side switches. To achieve ZVS for secondary side switches, as Fig.2(c) shows, the magnetizing inductance is proposed to be added into consideration, which is rarely studied in previous works. The polarity of i_{p_s} will be changed through injecting the magnetizing current, and ZVS can be realized for the secondary side switches.

As analyzed above, the utilizing of the magnetizing inductance can provide a possibility to achieve full load ZVS for DAB converter under SPS control, and through designing the mismatching point and magnetizing inductance, DAB converter can achieve ZVS for all switches at light load.

III. ZVS Analysis with Magnetizing Inductance

A. ZVS Condition Analysis Considering Magnetizing Inductance and Switch Junction Capacitors.

To achieve ZVS for all the switches, the energy in the inductive components must be high enough to charge/discharge the switch junction capacitors sufficiently. For the primary side, i_p will approach its maximum value when S_1 is turned off, and L_k then charges/discharges the capacitors.

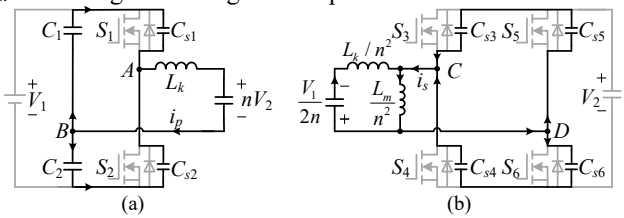

Fig. 3. Equivalent ZVS circuit. (a) The equivalent ZVS circuit after S_1 is turned off. (b) Equivalent ZVS circuit after S_3 and S_6 are turned off.

Fig.3(a) shows the equivalent ZVS circuit considering junction capacitors after S_1 is turned off. As illustrated, i_p charges C_2 and C_{s1}, and discharges C_1 and C_{s2}. The total energy includes three parts: the energy stored in L_k, energy in all the capacitors and the energy flowing into V_2. During the charging/discharging process, the sum of all energy in the junction capacitors is a constant value, while the energy of the inductor is decreased and fed back to secondary side. These energy relations can be expressed as

$$E_L(t_3) = E_L(t_4) + E_{feedback} = \frac{1}{2} L_k i_{p\_p}^2 \tag{1}$$

The relationship of leakage inductor current and capacitor voltage can be expressed as

$$i_p(t) = C_{s1}\frac{du_{s1}(t)}{dt} - C_{s2}\frac{du_{s2}(t)}{dt} = 2C_{s1}\frac{du_{s1}(t)}{dt} \tag{2}$$

where $u_{s1}(t)$ and $u_{s2}(t)$ are the voltages of switch junction capacitors for S_1 and S_2, respectively.

When ZVS resonant process is finished, the energy stored in L_k feeds back to V_2, which is calculated as

$$E_{feedback} = \int_{t_3}^{t_4} nV_2 \cdot i_p(t)dt \tag{3}$$

The switch junction capacitors will be charges/discharges sufficiently, in another word, the remaining energy of the inductor is greater than zero after the resonant process. Therefore, the range of i_{p_p} for ZVS realization of primary side switches can be obtained as (4) according to (1), (2) and (3).

$$i_{p\_p}(\varphi) \geq \sqrt{\frac{4nV_1V_2C_{s1}}{L_k}} \tag{4}$$

where φ is the phase-shift ratio of the two bridges, L_k is the leakage inductance.

For ZVS realization of the secondary side switches, the polarity of i_{p_s} needs to be considered. Fig.3(b) illustrates the equivalent ZVS circuit considering magnetizing inductor and the switch junction capacitors after S_3 and S_6 are turned off. As illustrated, the direction of i_s is changed through canceling i_p by injecting the magnetizing current. Therefore, the sufficient condition for secondary switches to achieve ZVS is

$$i_{p\_s}(\varphi) > 0 \tag{5}$$

B. ZVS Range Extension with Magnetizing Inductance

The power transfer of the proposed converter is expressed as

$$P(\varphi)=\frac{nV_1V_2\varphi(1-2\varphi)}{2L_kf} \tag{6}$$

where f is the switching frequency. To normalize the calculation, the base power can be defined when the phase-shift-ratio φ equals to 0.25 and the voltages are matched ($V_1 = 2nV_2$), which is expressed as

$$P_{base} = \frac{V_1^2}{32L_kf} \tag{7}$$

Then the normalized power by φ is shown as

$$P^*(\varphi) = \frac{P(\varphi)}{P_{base}} = 8G\varphi(1-2\varphi) \tag{8}$$

where G is the ratio of the voltages at two ports, and $G = 2nV_2/V_1$. The base current is defined as

$$I_{base} = \frac{P_{base}}{V_1} = \frac{V_1}{32L_kf} \tag{9}$$

According to the above analysis, i_{p_p} and i_{p_s} are the major concerns for the switches to realize ZVS. The normalized i_{p_p} can be calculated as

$$i^*_{p\_p}(\varphi) = \frac{i_{p\_p}(\varphi)}{I_{base}} = 16G\varphi - 4G + 4 \tag{10}$$

And the normalized i_{p_s} can be obtained in a similar way.

$$i^*_{p\_s}(\varphi) = \frac{i_{p\_s}(\varphi)}{nI_{base}} = 16\varphi + 4G(1+k_L) - 4 \tag{11}$$

where k_L is the ratio between the leakage inductance and the magnetizing inductance: $k_L = L_k/L_m$.

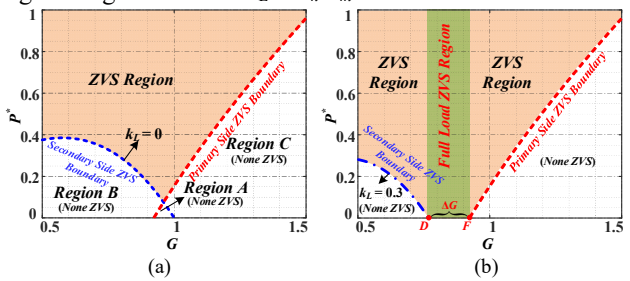

Fig. 4. ZVS range comparison. (a) ZVS range versus P^* and G with $k_L = 0$. (b) ZVS range versus P^* and G with $k_L = 0.3$.

According to (10) and (11), Fig.4 plots the ZVS range versus normalized power P^* and G, with different k_L. As Fig.4(a) shows, Region B cannot achieve ZVS for secondary side switches, Region C cannot achieve ZVS for primary side switches, and Region A cannot achieve ZVS for all the switches. So, at light load, none ZVS region will always occurs no matter how to design the gain G. This indicates that it is impossible to achieve ZVS at light load for all the switches under SPS control.

In order to achieve ZVS at light load for both side switches, the magnetizing current is considered, thus k_L is no longer equal to zero. As Fig.4(b) shows, ZVS range will be expanded when k_L increases from 0 to 0.3, and full load range ZVS can be achieved when G is in the range between point D to F. Namely, with the proper design of G and k_L, the DAB converter can be achieved full load range ZVS within variable gain range ΔG shown in Fig.4(b).

IV. Design Consideration to Achieve Full Load Range ZVS with Minimum RMS Current

As the analysis above, to achieve ZVS for all switches in full load range, G and k_L should be properly designed. Meanwhile, the RMS value of i_p and i_s need to be optimized to decrease the conduction loss. Since the working principle is symmetrical under different power direction, only the case of forward power transfer mode is analyzed.

A. Optimized Conversion Gain G design to Achieve ZVS for Primary Side Switches with Minimum Primary RMS Current

To achieve ZVS for the primary side switches, G should be properly designed to ensure that i_{p_p} is high enough to charge/discharge junction capacitors, and also to obtain a relatively lower RMS current. In addition, L_k and G should also guarantee the maximum power transfer. The normalized RMS current value of of i_p is expressed as

$$I^*_{p\_rms}(\varphi) = \frac{I_{p\_rms}(\varphi)}{I_{base}} = 4\sqrt{\frac{G^2 - 64G\varphi^3 + 48G\varphi^2 - 2G + 1}{3}} \tag{12}$$

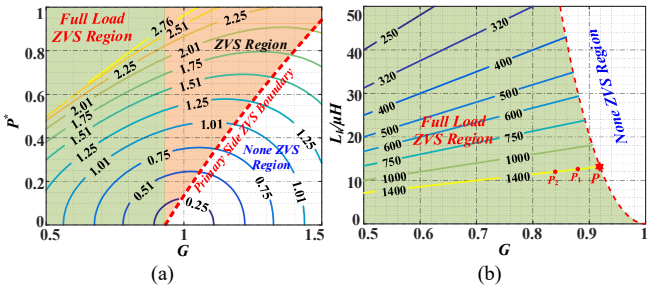

Fig. 5. L_k and G optimization (f = 250kHz). (a) The RMS value contour line versus G and P^*. (b) The maximum transferred power contour line versus L_k and G.

Fig.5(a) plots the RMS value contour line versus G and P^*, and the ZVS range is marked according to (4). As seen, in the full load ZVS region, for a given output power, the RMS current is decreased as G increases. So, to optimize RMS current, G should be designed as large as possible in full load ZVS region. Fig.5(b) illustrates the maximum transferred power contour line versus L_k and G. To satisfy the maximum transferred power, L_k should be designed according to the power curves as shown in Fig.5(b). Meanwhile, G should be designed as large as possible with light load ZVS. In this letter, the rated power of the prototype is set as 1000W. And the

maximum power is designed to be larger than the rated power about 40% to leave some power margins. Then, the recommended design is $G = 0.92$, $L_k = 13\mu H$, which is shown as point P in Fig.5(b).

B. Magnetizing Current Injection Optimization for ZVS of Secondary Side Switches.

For ZVS realization of secondary side switches, the magnetizing current should be properly designed to inject reactive energy for secondary switches. Meanwhile, the RMS value of i_s needs to be optimized to decrease the related loss. The normalized RMS current value of i_s is expressed as

$$I^*_{s\_rms}(\varphi) = \frac{I_{s\_rms}(\varphi)}{nI_{base}} = 4\sqrt{\frac{[16(3-4\varphi)\varphi^2 + (1+k_L)G - 2](1+k_L)G + 1}{3}} \tag{13}$$

Fig.6 plots $I^*_{s\_rms}$ versus P^* and k_L, and the ZVS range is marked according to (5). As Fig.6(a) shows, to achieve full load range ZVS for secondary side switches, k_L should be designed at full load ZVS region. As Fig.6(b) shows, in full load ZVS region, with a certain P^*, $I^*_{s\_rms}$ is decreased as k_L decreases. To optimize RMS current, k_L should be designed as small as possible in full load ZVS region. Therefore, k_L can be set as 0.1, which can achieve both full load range ZVS and relatively small RMS current.

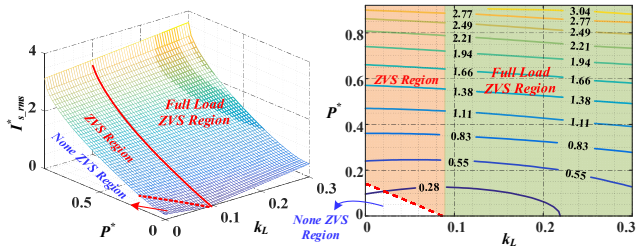

Fig. 6. $I^*_{s\_rms}$ versus P^* and k_L ($G = 0.92$). (a) 3D plots. (b) Contour line plots.

V. Experimental Results and Comparison

A 1000W prototype of a GaN-based DAB converter is built to verify the effectiveness of the proposed solution, which is shown in Fig.7. The detailed specifications are designed according to Fig.5 and Fig.6, which are shown in TABLE I. Meanwhile, the parameters for conventional DAB design are also included.

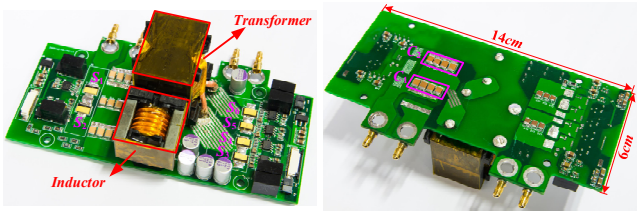

Fig. 7. The experimental prototype.

Fig.8 illustrates the ZVS waveforms of the primary side switch and the secondary side switch at no load condition with the proposed method. v_{gs1} and v_{gs3} are the driving signals of S_1 and S_3, respectively. v_{ds1} and v_{ds3} are the voltage across S_1 and S_3, respectively. i_p and i_s are the primary side current and secondary side current of the transformer, respectively. As Fig.8 (a) shows, when S_1 is turned on, i_p is negative, which discharges the junction capacitor of S_1, and ZVS is achieved. As Fig.8(b) shows, when S_3 is turned on, i_s is positive, which discharges the junction capacitor of S_3, and ZVS is achieved. Note that, the Chanel M is the math utility of the scope, and the calculation formula is $(i_p - i_s/n)$, which represents the magnetizing current. As seen, the amplitude of i_{Lm} is slightly higher than i_p, which can change the polarity of i_s, and achieve ZVS for secondary side switches.

TABLE I Parameters of the prototype

Item	Detail (Proposed)	Detail (Conventional)
Rated Power (P)	$1000W$	
Primary side Voltage (V_1)	$400V$	
Secondary side Voltage (V_2)	$48V$	
Leakage Inductance (L_k)	$13\mu H$	
Magnetizing Inductance (L_m)	$130\mu H$ ($k_L = 0.1$)	Ignored ($k_L \approx 0$)
Turns Ratio (n)	23:6 ($G = 0.92$)	25:6 ($G = 1$)
Switching Frequency (f)	$250kHz$	
Half bridge capacitance (C_1, C_2)	$4\mu F$	
Primary side switches (S_1, S_2)	GS66508T	
Secondary side switches (S_3~S_6)	GS61008T	

Fig.8(c) and Fig.8(d) illustrate the ZVS waveforms of the primary side switch and the secondary side switch at no load condition with the conventional method. As seen, both the primary side and secondary side switches are suffering hard switching, because i_p and i_s are so small that the energy stored in the inductor cannot charge/discharge the junction capacitor of switches sufficiently.

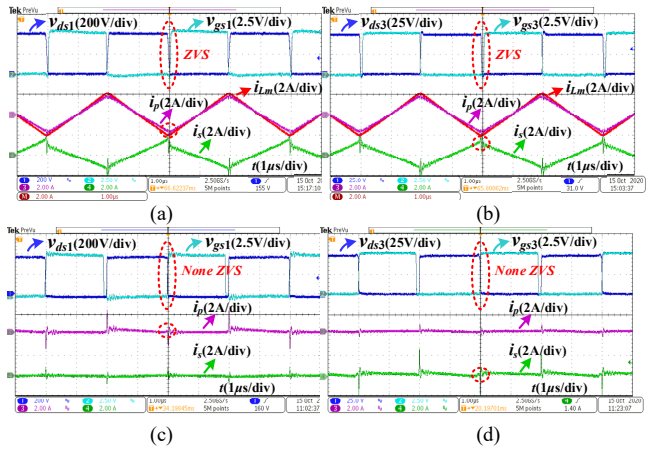

Fig. 8. ZVS waveforms at no load. (a) Primary side switch with proposed method. (b) Secondary side switch with proposed method. (c) Primary side switch with conventional method. (d) Secondary side switch with conventional method.

Fig.9 shows the ZVS waveforms with two methods when the output power is 1000W. As seen, when the converter works at heavy load condition, both two methods can achieve ZVS sufficiently for all switches.

Fig.10(a) shows the measured RMS current of i_p with different G, and the corresponding power points P_1 and P_2 are denoted in Fig.5. As for the conventional DAB converter, G is equal to 1, and the RMS current is the smallest. However, when G = 1, full load rang ZVS cannot be achieved. When G is decreased, full load range ZVS can be achieved. But, smaller G will lead to higher RMS current. So, G should be as large as possible if full load range ZVS is achieved. Then the optimal point P ($G = 0.92$) can be selected for obtaining both full load range ZVS and relatively small RMS current. As for the

transformer secondary side RMS current I_{s_rms} shown in Fig.10(b), its value is almost the same with different G.

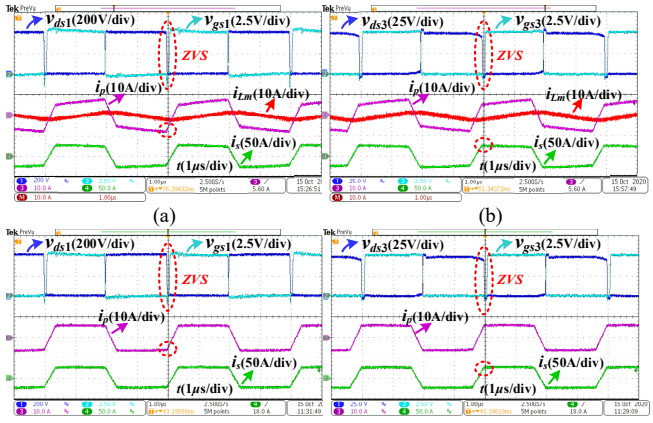

Fig. 9. ZVS waveforms when P = 1000W. (a) Primary side switch with proposed method. (b) Secondary side switch with proposed method. (c) Primary side switch with conventional method. (d) Secondary side switch with conventional method.

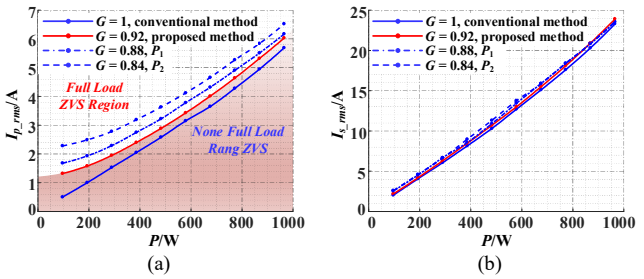

Fig. 10. The measured RMS current of i_p and i_s with different G. (a) The measured I_{p_rms}. (b) The measured I_{s_rms}.

The loss breakdown comparisons of the converter between the proposed method and the conventional method at different loads are shown in Fig.11. As Fig.11(a) shows, when the converter works at light load (100W), the total loss of the conventional method is higher than that of the proposed method about 7W, which is mainly caused by hard switching loss, leading to low efficiency at light load. As Fig.11(b) shows, when the converter works at heavy load condition (1000W), the power loss with the proposed method is higher than that of the conventional method about 5W, which is mainly caused by the increased conduction and copper loss. The loss difference between the two methods accounts for only 0.5% of the total power at 1000W.

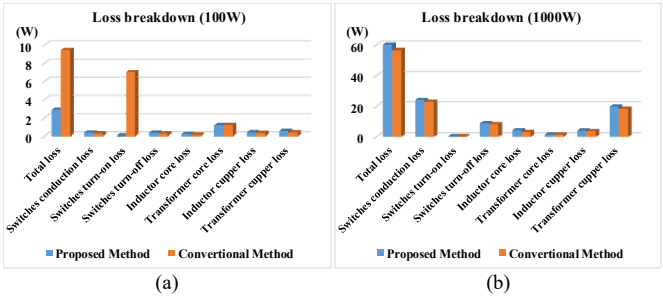

Fig. 11. Loss breakdown comparisons. (a) At light load (100W) (b) At heavy load (1000W).

Fig.12 plots the efficiency of the proposed method and the conventional DAB converter under SPS control. As seen, when working at light load, the proposed method has better efficiency than the conventional DAB converter, which is mainly caused by losing ZVS for the conventional method. And at heavy load, the efficiency of the proposed method is slightly lower than that of the conventional DAB converter because the injected magnetizing current could slightly increase the conduction loss.

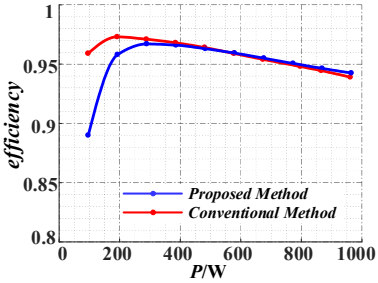

Fig. 12. Efficiency comparison between the proposed method and the conventional method.

TABLE II Comparison with other works

Item	Full load range ZVS	Light load efficiency	
		10% rated power	20% rated power
Proposed Method	Yes	96%	97.3%
Conventional Method	No	89%	96%
Method in [11]	No	<94%	96%
Method in [12]	No	96%	94%

There are also some works on the improvement of the light load efficiency. TABLE II illustrates the ZVS range and the light load efficiency at different working points with different methods. As seen, only the proposed method can achieve full load range ZVS with SPS control scheme. Besides, with the proposed method, the efficiency at 10% and 20% of the rated power is higher than that of other works.

VI. Conclusions

This letter proposed a method to enhance the light-load efficiency for DAB converter. With the consideration of magnetizing inductance, full load range ZVS can be achieved under SPS control. The voltages gain point and the magnetizing inductance are specially designed to achieve full load range ZVS for all switches considering switch junction capacitors, and the efficiency at light load is improved. ZVS model analysis, ZVS range and design consideration are presented in this letter. The experimental results from a 250 kHz, 400/48V, 1000W prototype have verified that the performance of the DAB converter with proposed method is enhanced. Beside, by comparing the proposed method with other recent works, it shows the benefit of the proposed method. Meanwhile, the basic concept of the proposed method can also be applied into other types DAB converter for achieving better features, such as full bridge DAB converter, push-pull DAB converter, the three phase DAB converter, etc.

References

[1] M. Ryu, H. Kim, J. Baek, H. Kim and J. Jung, "Effective Test Bed of 380-V DC Distribution System Using Isolated Power Converters," IEEE Transactions on Industrial Electronics, vol. 62, no. 7, pp. 4525-4536, July 2015.

[2] H. Shi *et al*., "Minimum-Backflow-Power Scheme of DAB-Based Solid-State Transformer with Extended-Phase-Shift Control," *IEEE Transactions on Industry Applications*, vol. 54, no. 4, pp. 3483-3496, July-Aug. 2018.

[3] T. Zhao, G. Wang, S. Bhattacharya and A. Q. Huang, "Voltage and Power Balance Control for a Cascaded H-Bridge Converter-Based Solid-State

Transformer," *IEEE Transactions on Power Electronics*, vol. 28, no. 4, pp. 1523-1532, April 2013.

[4] J. Lee, H. Kim and J. Jung, "Enhanced Dual-Active-Bridge DC-DC Converter for Balancing Bipolar Voltage Level of DC Distribution System," *IEEE Transactions on Industrial Electronics*.

[5] B. Zhao, Q. Song, W. Liu and Y. Sun, "Overview of Dual-Active-Bridge *hacve*olated Bidirectional DC–DC Converter for High-Frequency-Link Power-Conversion System," *IEEE Transactions on Power Electronics*, vol. 29, no. 8, pp. 4091-4106, Aug. 2014.

[6] X. Sun, H. Wang, L. Qi and F. Liu, "Research on Single Stage High Frequency Link SST Topology and Its Optimization Control," *IEEE Transactions on Power Electronics*, doi: 10.1109/TPEL.2020.2964065.

[7] P. Liu, C. Chen, S. Duan and W. Zhu, "Dual Phase-Shifted Modulation Strategy for the Three-Level Dual Active Bridge DC–DC Converter," *IEEE Transactions on Industrial Electronics*, vol. 64, no. 10, pp. 7819-7830, Oct. 2017.

[8] Z. Guo and D. Sha, "Dual-Active-Bridge Converter with Parallel-Connected Full Bridges in Low-Voltage Side for ZVS by Using Auxiliary Coupling Inductor," *IEEE Transactions on Industrial Electronics*, vol. 66, no. 9, pp. 6856-6866, Sept. 2019.

[9] M. N. Kheraluwala, R. W. Gascoigne, D. M. Divan and E. D. Baumann, "Performance characterization of a high-power dual active bridge DC-to-DC converter," *IEEE Transactions on Industry Applications*, vol. 28, no. 6, pp. 1294-1301, Nov.-Dec. 1992.

[10] J. Riedel, D. G. Holmes, B. P. McGrath and C. Teixeira, "Maintaining Continuous ZVS Operation of a Dual Active Bridge by Reduced Coupling Transformers," *IEEE Transactions on Industrial Electronics*, vol. 65, no. 12, pp. 9438-9448, Dec. 2018.

[11] A. Jafari, M. S. Nikoo, F. Karakaya and E. Matioli, "Enhanced DAB for Efficiency Preservation Using Adjustable-Tap High-Frequency Transformer," *IEEE Transactions on Power Electronics*, vol. 35, no. 7, pp. 6673-6677, July 2020.

[12] P. Liu and S. Duan, "A ZVS Range Enhancement Strategy for the DAB Converter by Using Blocking Capacitors," *IEEE Journal of Emerging and Selected Topics in Power Electronics*, doi: 10.1109/JESTPE.2020.3016052.